

Utah State University

DigitalCommons@USU

Geology

U.S. Government Documents (Utah Regional
Depository)

5-28-1986

Simulating a Large Wasatch Front, Utah, Earthquake Using Small Earthquake Recordings as Green's Functions

United States Department of Defense, Air Force Geophysics Laboratory

Follow this and additional works at: https://digitalcommons.usu.edu/govdocs_geology



Part of the [Geophysics and Seismology Commons](#)

Recommended Citation

United States Department of Defense, Air Force Geophysics Laboratory, "Simulating a Large Wasatch Front, Utah, Earthquake Using Small Earthquake Recordings as Green's Functions" (1986). *Geology*. Paper 1.

https://digitalcommons.usu.edu/govdocs_geology/1

This Report is brought to you for free and open access by the U.S. Government Documents (Utah Regional Depository) at DigitalCommons@USU. It has been accepted for inclusion in Geology by an authorized administrator of DigitalCommons@USU. For more information, please contact digitalcommons@usu.edu.



FEB 9 1987

D301-45/4: 86-0120

AFGL-TR-86-0120
ENVIRONMENTAL RESEARCH PAPERS, NO. 956

COMPLETED

33

Simulating a Large Wasatch Front, Utah, Earthquake Using Small Earthquake Recordings as Green's Functions

JANET C. JOHNSTON

ORIGINAL



28 May 1986



Approved for public release; distribution unlimited.



Am/nlk



EARTH SCIENCES DIVISION

PROJECT 7600

AIR FORCE GEOPHYSICS LABORATORY

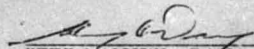
HANSCOM AFB, MA 01731

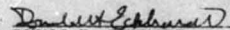
BEST COPY AVAILABLE

IN-HOUSE REPORTS

This technical report has been reviewed and is approved for publication.

FOR THE COMMANDER


HENRY A. OSSING, Chief
Solid Earth Geophysics Branch


DONALD H. ECKHARDT
Director
Earth Sciences Division

This document has been reviewed by the ESD Public Affairs Office (PA) and is releasable to the National Technical Information Service (NTIS).

Qualified requestors may obtain additional copies from the Defense Technical Information Center. All others should apply to the National Technical Information Service.

If your address has changed, or if you wish to be removed from the mailing list, or if the addressee is no longer employed by your organization, please notify AFGL/DAA, Hanscom AFB, MA 01731. This will assist us in maintaining a current mailing list.

BEST COPY AVAILABLE

UNCLASSIFIED
SECURITY CLASSIFICATION OF THIS PAGE

REPORT DOCUMENTATION PAGE

1a REPORT SECURITY CLASSIFICATION Unclassified		1b RESTRICTIVE MARKINGS	
2a SECURITY CLASSIFICATION AUTHORITY		3 DISTRIBUTION/AVAILABILITY OF REPORT Approved for Public release; Distribution unlimited	
2b DECLASSIFICATION/DOWNGRADING SCHEDULE			
4 PERFORMING ORGANIZATION REPORT NUMBER(S) AFGL-TR-86-0120 ERP, No. 956		5 MONITORING ORGANIZATION REPORT NUMBER(S)	
6a NAME OF PERFORMING ORGANIZATION Air Force Geophysics Laboratory	6b OFFICE SYMBOL (if applicable) LWH	7a NAME OF MONITORING ORGANIZATION	
6c ADDRESS (City, State, and ZIP Code) Hanscom AFB Massachusetts 01731		7b ADDRESS (City, State, and ZIP Code)	
8a NAME OF FUNDING, SPONSORING ORGANIZATION	8b OFFICE SYMBOL (if applicable)	9 PROCUREMENT INSTRUMENT IDENTIFICATION NUMBER	
8c ADDRESS (City, State, and ZIP Code)		10 SOURCE OF FUNDING NUMBERS	
		PROGRAM ELEMENT NO 62101F	PROJECT NO 7600
		TASK NO 03	WORK UNIT ACCESSION NO 04
11 TITLE (Include Security Classification) SIMULATING A LARGE WASATCH FRONT, UTAH, EARTHQUAKE USING SMALL EARTH- QUAKE RECORDINGS AS GREEN'S FUNCTIONS			
12 PERSONAL AUTHOR(S) Janet C. Johnston			
13a TYPE OF REPORT Scientific Interim	13b TIME COVERED from Sept. 83 to Oct. 85	14 DATE OF REPORT (Year, Month, Day) 28 May 1986	15 PAGE COUNT 60
16 SUPPLEMENTARY NOTATION			
17 COSATI CODING		18 SUBJECT TERMS (Continue on reverse if necessary and identify by block number)	
FIELD	GROUP	Utah earthquakes, Synthetic waveforms, Green's function addition, Wasatch Front earthquakes, Seismic hazard, Earthquake prediction	
19 ABSTRACT (Continue on reverse if necessary and identify by block number) Several earthquake recordings at Golden, Colorado in the magnitude range 4-6, were digitized and were used to investigate the feasibility of adding them together to simulate a larger earthquake (magnitude 7.0-7.5). The test path of the Wasatch Front, Utah to the WSSN station at Golden was selected (distance = 400-500 km). The hypothetical causative fault was given dimensions on the order of 45 km long by 20 km wide and was divided into "cells," representative in size to the "seed" events rupture dimensions and with other variations. The results were evaluated by total energy and amplitude criteria. The final waveforms were judged to be adequate predictions at the lower frequency end of the spectra. The high frequency content was controlled by the spectra of the seed earthquakes whose magnitudes were too large to adequately reproduce the Green's function response at these frequencies. It is recommended that this technique be used at smaller distance ranges or at stations whose sensitivity is set high enough so as to record the smaller magnitude earthquakes, more representative of impulse responses at all frequencies.			
20 DISTRIBUTION/AVAILABILITY OF ABSTRACT <input type="checkbox"/> UNCLASSIFIED UNLIMITED <input checked="" type="checkbox"/> SAME AS RPT <input type="checkbox"/> DTIC USERS		21 ABSTRACT SECURITY CLASSIFICATION Unclassified	
22a NAME OF RESPONSIBLE INDIVIDUAL Janet C. Johnston		22b TELEPHONE (Include Area Code) 617-377-3767	22c OFFICE SYMBOL AFGL/LWH

DD FORM 1473, 84 MAR

83 APR edition may be used until exhausted
All other editions are obsoleteSECURITY CLASSIFICATION OF THIS PAGE
UNCLASSIFIED

BEST COPY AVAILABLE

Preface

John Cipar summarized the documentation on the crustal structure between Golden, Colorado and the Wasatch Front Zone. The author thanks Dr. Cipar for his help in making the signal processing software operational at AFGL.

Dr. Otto Nuttli provided some useful comments on the composite earthquake results.

Dr. Lawrence Hutchings provided several references, including his doctoral thesis. The author is grateful to Dr. Hutchings for sharing his insight into the problem.

The author also thanks TSgt Sandra Botka for her assistance in the preparation of the manuscript.

Contents

1. INTRODUCTION	1
2. TEST AREA	1
2.1 Wasatch Front Earthquakes	2
2.2 Crustal Structure	2
3. THEORETICAL BACKGROUND AND HISTORY OF GREEN'S FUNCTION	7
4. GREEN'S FUNCTION ADDITION OF SMALL EARTHQUAKES	12
4.1 Source Parameters Estimates and Conversions	12
4.2 Geometric Approach	16
4.2.1 Rupture Velocity Sensitivity	16
4.2.2 Initial Cracking Position	29
4.2.3 Noise Accumulation	29
4.3 Energy and Moment Approach	29
4.3.1 Incoherent Rupture	32
5. DISCUSSION	32
6. CONCLUSIONS	42
REFERENCES	45
BIBLIOGRAPHY	49

1. Earthquake Source Zones for Seismic Hazard Estimates (Johnston, 1983)	4
2. Selected Structural Models from the Basin and Range Eastward to the Great Plains. First number or single number is the P-wave velocity, second is the S-wave velocity. Single lines are layer boundaries; double line is the Moho; hatchures indicate a low velocity layer. Arrows indicate a gradual increase in velocity. Letters below each profile indicate references in Table 3	7
3. Crustal Q_0 as a Function of Depth	9
4. Location of Earthquakes Used in the Study. Single numbers refer to events in Table 1. Distances to Golden, Colorado, are listed in kilometers	13
5. Digitized Records of Seed Earthquakes Used to Create Composite Earthquake, a) Is a Short Period Record; Others are Long Period Records	17
6. Spectra of Seed Earthquakes as Recorded at Golden WWSSN	20
7. Model of Earthquake Rupture Process. After crack initiation, cells rupture in order of closest distances. Amplitude scaling is optional	25
8. a) Vertical Fault Model b) Dipping Fault Model	26
9. Original Record, $V_{rup} = 2.0$ km/sec, 2.5 km/sec, 1.7 km/sec, and $V_{rup} = 2.0$ km/sec with Number of Seed Events = 134 for a) Event 3 and b) Event 5. Cracking starts at edge of fault	27
10. Magma Earthquake Records and Spectra Before Stacking and After (Model: 45 km x 29 km, $V_{rup} = 2.0$ km/sec, NS = 67). Cracking starts at edge of fault	30
11. Effect of Central Crack Initiation: a) Event 3, Z Component; and b) Event 5, Z Component	31
12. Composite Earthquakes from Wasatch Front as Predicted to be Measured at Gol. Short period record event number 1 high-pass filtered at 0.25 Hz. Long period record event number 4 high-pass filtered at 0.025 Hz	33
13. Spectra of Composite Events. Events 1 and 4 have been filtered to remove noise	36
14. a) Event 3 Normal Composite Earthquake b) Event 3 Composite Earthquake with Central Barrier on Fault	41
15. Two Recordings at Golden WWSSN a) Truckee Earthquake Arrivals (as analyzed by Helmlinger and Engen, 1980) b) Richfield Earthquake (this study)	43

Tables

1. Source Data for Chosen Earthquake Records	3
2. Recurrence Relations for Zonation Scheme of Figure 1 (Johnston 1988)	5
3. References for Figures 2 and 3	8
4. Previous Investigations of Green's Functions Used to Synthesize Earthquakes	11
5. Empirically Based Magnitude - Energy, Moment Pairs with Estimated Rupture Dimensions	15
6. Composite Parameters for Waveforms in Figure 12	32

Simulating a Large Wasatch Front, Utah, Earthquake Using Small Earthquake Recordings as Green's Functions

1. INTRODUCTION

The effects of long and short period vibrations on missile systems and their support facilities have been a concern of the Air Force for some time. Such in-ground vibrations can be caused by nuclear detonations, conventional weapons, large chemical explosions and earthquakes. These sources can produce significant ground motion even over distances of hundreds of kilometers from a site. Lately, there has been a significant amount of research on the use of small earthquake recordings as Green's functions for the synthesis of larger events (Section 2.3). In this report such a method is used to predict ground motion from an earthquake at a station that has not had an on-scale recording of a major event from the particular source region. This report contains a description of the method and a chosen data set. It includes the results of several sensitivity experiments as a test of the feasibility of the method for Air Force needs.

2. TEST AREA

The general area of concern for this study is the central and western United States. Initially a single test site and single source region are used for a case study.

(Received for publication 27 May 1986)

The test receiver location of Golden, Colorado, the site of a WSSN (World-Wide Standard Seismograph Network) station, was chosen. The source region for the study is the Wasatch Front in Utah, the scene of several moderate to large earthquakes.

2.1 Wasatch Front Earthquakes

The Wasatch Front is a segment of the Intermountain Seismic Belt, which is a 1300 km long north-south zone of generally normal faults and high seismicity. The zone marks the transition between the basin and range province to the west and the Colorado Plateau to the east. Earthquake activity along this area is generally diffuse with shallow focal depths (less than 15 km), often occurs in swarms, and generally results in fault plane solutions which exhibit east-west extension¹. Although many Wasatch Front earthquakes are located to the east of this physiographic boundary, it is generally recognized that the Intermountain Seismic Belt separates two continental sub-plates. As such, earthquakes from this region do not exhibit purely "intraplate" source characteristics. Table 1 lists the earthquake records used in this study. All were from the WSSN station at Golden, digitized by hand. Size estimates of the maximum magnitude earthquake vary from the northern part of the Wasatch Front to the southern part. The latter possesses the higher seismic hazard (see Figure 1, Table 2). Historically the largest event to occur in Utah was the 1934 Hansel Valley earthquake ($M = 6.6$). Typical design criteria for critical structures often choose a maximum earthquake size that is 1/2 to 1 magnitude higher than the largest historical event. According to the calculations of Battis² such an event may have a return period of approximately 250 years. Geological data suggest 100 to 200 years although no event of that size has occurred since the area was populated (~1850). This study models a 7.0 - 7.5 M_L earthquake. Seismic waves from the Wasatch Front traveling to Golden cross two geologic provinces: the Colorado Plateau and South Rocky Mountains.

2.2 Crustal Structure

The Wasatch Fault lies at the eastern edge of the Basin and Range tectonic province of western North America. The Basin and Range is characterized by thin crust (30-35 km), low P_n velocity (7.8 km/sec), and recent extensional tectonics^{3,4}.

1. Smith, R.B., (1975) "Seismicity and Earthquake Hazards of the Wasatch Front, Utah," Hearing before the Committee on Aeronautical and Space Sciences, United States Senate, 94th Congress, U.S. Government Printing Office, Washington, D.C.
2. Battis, J.C., (1982) "Seismic Hazard Study for Utah," AFGL-TR-82-0319, ADA129238.
3. Hamilton, W., and Myers, W.B. (1966) Cenozoic Tectonics of the Western United States, Reviews of Geophysics, 4(No. 4):509-549.
4. Priestley, K., and Brune, J. (1978) Surface Waves and the Structure of the Great Basin of Nevada and Western Utah, J. Geophys. Res., 83(No. B5):2265-2272.

Table 1. Source Data for Chosen Earthquake Records

EVT NO.	DATE M-D-Y	TIME (GMT)	LOCATION (DEGREES)		MEASURED	CONVERTED	RECORDS	DIST (KM)	DEPTH (KM)	FAULT PLANE ESTIMATES* (AZ AND DIP)
			LAT	LONG	MAG	MAG M _s				
1	06-02-72	03:15	38.7	-112.1	4.6 M _b , 4.0 M _L	2.7	SHORT PERIOD Z	592	5(ISC)	170, 86W; 275, 15N
2	03-17-66	11:47	41.6	-111.6	4.6 M _L	3.7	LONG PERIOD Z	567	40(ISC)	
3	10-04-67	10:20	38.5	-112.1	5.3 M _L , 5.2 M _b	4.7	LONG PERIOD NS, EW, Z	597		170, 86W; 95, 15N
4	10-11-77	07:56	40.5	-110.5	4.8 M _b , 4.7 M _L	3.9	LONG PERIOD NS, EW, Z	446	3-6(ISC, NEIS)	
5	09-05-62	16:04	40.7	-112.1	5.2 M _L , 5.0 M _b	4.7	LONG PERIOD Z	584		330, 30NE; 17, 60SW

*DOSER AND SMITH, 1982

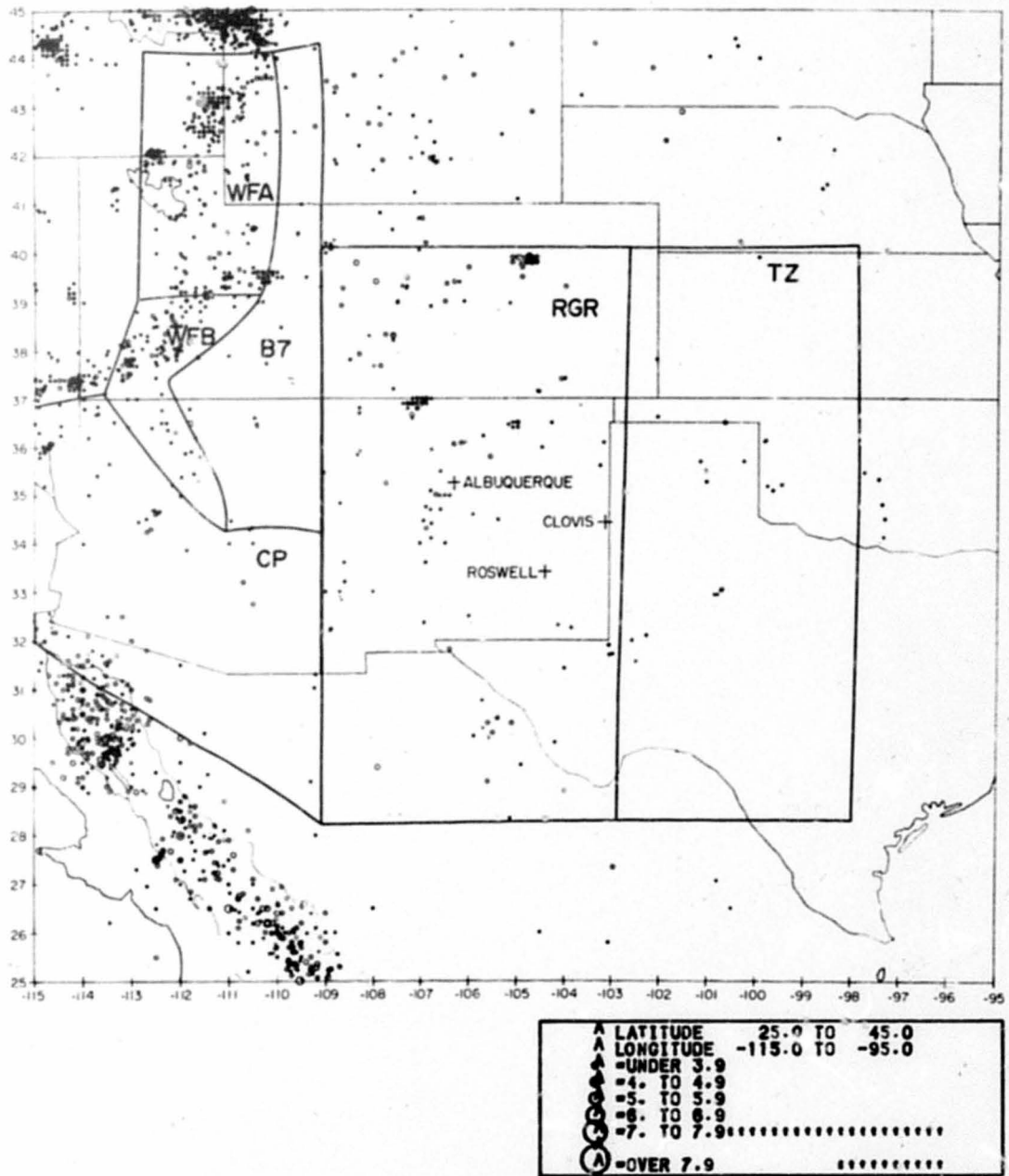


Figure 1. Earthquake Source Zones for Seismic Hazard Estimates (Johnston, 1983)

Table 2. Recurrence Relations for Zonation Scheme of Figure 1 (Johnston 1983)

Source Zone	Area (km) ²	Log N _c [*] = A - B M _L	Min M _L	Max M _L	Return Period of M _L Max (years)
TZ	6.15 × 10 ⁷	2.2 0.7	4.0	6.5	223
RGR	7.38 × 10 ⁵	3.7 0.8	4.0	7.0	79
B7	1.86 × 10 ⁵	4.2 1.0	4.0	6.75	354
WFA	6.56 × 10 ⁴	3.3 0.8	4.0	7.0	200
WFB	1.29 × 10 ⁵	2.3 0.5	4.0	7.75	38
• CP	3.5 × 10 ⁵	4.2 1.0	4.0	7.0	630

*N_c = cumulative number of events per annum of magnitude greater than or equal to M_L for each source zone (not normalized to area).

5

Eastward of the Wasatch Fault lies the Colorado Plateau, an uplifted area of thick crust (40-42 km) and low P_n velocity (7.8 km/sec) that has been relatively stable tectonically since Paleozoic times^{5,6,7}.

Keller et al.⁸ infer a major mantle σ_p jump along the transition zone between the Basin and Range and Colorado Plateau. Their interpretation of seismic refraction measurements indicates a crustal thickness of about 25 km and an abnormally low P_n velocity of 7.5 km/sec in a zone 80 km wide centered on the Wasatch Fault. East and west from this zone, the crust thickens and P_n velocities increase as outlined above.

The WSSN station at Golden, Colorado, (GOL) is located near the eastern edge of the southern Rocky Mountains, approximately 400 km from the Wasatch Fault. The crust thickens from approximately 48 km in the central part of the mountain range to over 50 km in the Front Range near Golden; P_n velocity is 7.9 km/sec^{9,10}. These variations in crustal structure are best illustrated by a west-east profile of crustal models (Figure 2). References for these models are listed in Table 3. Note especially the Moho upwarp and low P_n velocities in the transition zone, the area of the Wasatch Fault zone.

Depth to the low velocity zone in the western United States is measured as 60-70 km from body wave travel times¹¹, body waveforms¹², and surface waves⁴. Biswas and Knopoff¹³ inverted long-period surface data between Dugway, Utah and Golden, Colorado, finding that the best estimate of S-wave velocity and thickness of the mantle above the low velocity zone (lid) is 4.45 km/sec and 35 km, respectively.

5. Bucher, R.L., and Smith, R.B. (1971) Crustal Structure of the Eastern Basin and Range Province and the Northern Colorado Plateau from Phase Velocities of Rayleigh Waves, in *The Structure and Physical Properties of the Earth's Crust*, John G. Heacock, ed., Geophysical Monograph 14, AGU, Washington, D.C.
6. Keller, G.R., Braile, L.W., and Morgan, P. (1979) Crustal Structure, Geophysical Models and Contemporary Tectonism of the Colorado Plateau, *Tectonophysics*, 61:131-147.
7. Thompson, G.A., Zoback, M.L. (1979) Regional Geophysics of the Colorado Plateau, *Tectonophysics*, 61(No. 1-3):149-181.
8. Keller, G.R., Smith, R.B., and Braile, L.W. (1975) Crustal Structure Along the Great Basin - Colorado Plateau Transition from Seismic Refraction Studies, *J. Geophys. Res.*, 80(No. 8):1093-1098.
9. Jackson, W.H., and Pakiser, L.C. (1965) Seismic Study of Crustal Structure in the Southern Rocky Mountains, *U.S. Geological Survey Prof. Paper 525D*, pp. D85-D92.
10. Prodehl, C., and Pakiser, L.C. (1980) Crustal Structure of the Southern Rocky Mountains from Seismic Measurements, *Bull. Seismol. Soc. Am.*, 91:147-155.
11. Archambeau, C.B., Flinn, E.A., and Lambert, D.G. (1969) Fine Structure of the Upper Mantle, *J. Geophys. Res.*, 74(No. 25):5825-5865.
12. Burdick, L.J. (1977) *Broad-Band Seismic Studies of Body Waves*, Ph.D. Thesis, California Institute of Technology.
13. Biswas, N.N., and Knopoff, L. (1974) The Structure of the Upper Mantle under the United States from the Dispersion of Rayleigh Waves, *GJRS*, 36(No. 3):515-539.

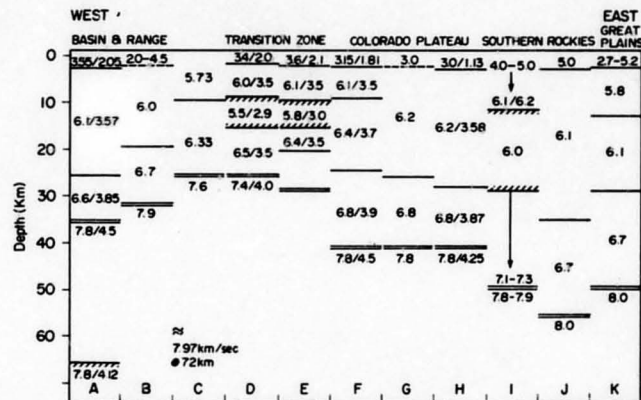


Figure 2. Selected Structural Models from the Basin and Range Eastward to the Great Plains. First number or single number is the P-wave velocity, second is the S-wave velocity. Single lines are layer boundaries; double line is the Moho; hatching indicates a low velocity layer. Arrows indicate a gradual increase in velocity. Letters below each profile indicate references in Table 3

Anelastic attenuation measurements are much sparser than velocity results and considerably more scattered. Results of three studies are presented in Figure 3. In both the Colorado Plateau and the Basin and Range, a low-Q upper crust is underlain by a high Q lower crust. The CIT 112 model is a world-wide average of long-period surface wave Q measurements. Clearly, more work is needed to adequately define seismic wave attenuation on a regional basis.

3. THEORETICAL BACKGROUND AND HISTORY OF GREEN'S FUNCTION APPROACH

The concept of earthquake size is multi-dimensional. Several parameters, such as magnitude and intensity, are popularly used to give some relative scale for the measurement of seismic events; however, a single measurement cannot adequately characterize such a dynamic process. This study utilizes many properties of an earthquake such as rupture velocity, fault length, fault width, fault slip, stress drop, propagation history, earthquake moment, earthquake energy and finally earthquake magnitude.

Table 3a. References for Figure 2

Profile	Investigator	Method/Model
A	Priestley and Brune, 1978	surface wave dispersion
B	Hill and Pakiser, 1967	P-wave refraction (in Basin and Range)
C	Berg et al., 1960	P-wave refraction
D	Keller et al., 1975	P- and S-wave refraction (Model A)
E	Braile et al., 1974	P- and S-wave refraction (Model 1)
F	Keller et al., 1976	surface wave dispersion (N. Colorado Plateau)
G	Roller, 1965	P-wave refraction
H	Bucher and Smith, 1971	surface wave dispersion (Model C7)
I	Prodehl and Fakiser, 1980	P-wave refraction (Lumberton to Sinclair)
J	Jackson and Pakiser, 1965	P-wave refraction (Climax model)
K	Jackson et al., 1963	P-wave refraction (Model A)

Table 3b. Crustal Q Measurements, References for Figure 3

Profile	Investigator	Method/Model
A	Archambeau et al., 1969	CIT 112
B	Bache et al., 1978	NTS-ALQ
C	Bache et al., 1978	NTS-TUC
D	Cheng and Mitchell, 1981	Colorado Plateau
E	Cheng and Mitchell, 1981	Basin and Range

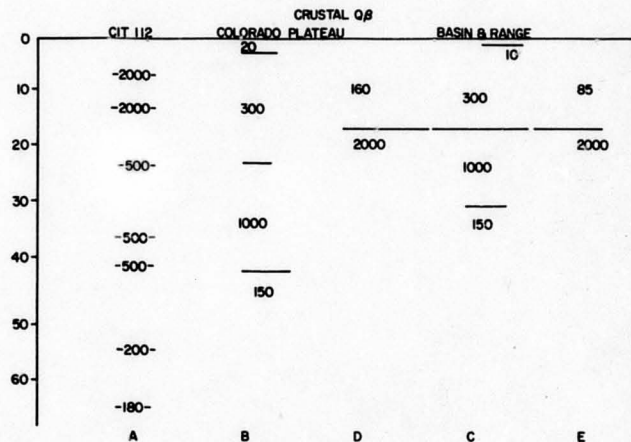


Figure 3. Crustal Q as a Function of Depth

The seismic moment, M_0 , which can be measured from the amplitude spectrum at very long periods, represents, more than any of the other size estimates mentioned above, the actual physical dimensions of an earthquake. The fault length, L , and width, W , and average fault displacement, \bar{D} , are related to the seismic moment by the rigidity modulus, μ , by the equation

$$M_0 = \mu L W \bar{D} \quad (\text{see Aki and Richards}^{14})$$

The mechanics of fault rupture can be quite complicated. The entire area of a fault involved in the rupture does not instantaneously slip; rather, a portion starts the fracture and this can propagate with a certain rupture velocity throughout the earthquake fault area. It can stop and restart with many variations (see, for example,

14. Aki, K., and Richards, P.G. (1979) Quantitative Seismology, Theory and Methods, Vol. I, W.H. Freeman and Co., San Francisco, California.

Joyner and Boore¹⁵ for a description of rupturing during the Parkfield earthquake). If we consider separately a precise location in space and time along a rupturing front (whatever configuration that might have), we could reduce a complicated rupturing history to a series of unit impulses. The resulting displacement field from such a source is the elastodynamic Green's function¹⁴. Mathematically it can be represented as follows: A displacement at X caused by a displacement discontinuity

$$[\bar{U}(\xi, \tau)]$$

across Σ is

$$U_n(\bar{x}, t) = \iint_{\Sigma} m_{pq} * G_{np,q} d\Sigma \quad (\text{see Aki and Richards}^{14})$$

where * denotes convolution:

$$\Sigma G_{np,q} \text{ is the elastodynamic Green's function, and } m_{pq} \text{ is the moment tensor.}$$

The model in this paper uses the recordings at the observation point which incorporate the WWSSN instrument response in the integrated above. That is, these recordings are the responses to an impulse rupture at the fault (along Σ). Rather than modeling the impulses along the source, and then having to compensate for effects along the ray path, the aim of this study is to produce a time history of a large event recorded at a distant site by approximating the unit impulse response at distance, due to a rupturing area, by recordings of small earthquakes. These will be referred to as the "seed" events. In other words, small earthquakes are being added together as components of one large earthquake.

Variations of the method have been used by previous investigators (see Table 4). Hartzel¹⁶ used two aftershocks of the 1940 Imperial Valley event recorded at El Centro scaled for moment by a simple linear multiplication to add up to the total moment of the basic event. Heaton¹⁷ used synthetic Green's functions for a halfspace to model near-field motion from the 1971 San Fernando earthquake. Kanamori¹⁸ combined the Borrego

15. Joyner, W.B. and Boore, D.M. (1985) "On Simulating Large Earthquakes by Green's Function Addition of Smaller Earthquakes," manuscript submitted to the Proceedings of the 5th Maurice Ewing Symposium - Earthquake Source Mechanics, May 19-23, (1985) Harriman, N.Y.
16. Hartzel, S.H. (1978) Earthquake Aftershocks as Green's Functions, Geophys. Res. Letts., 5(No. 1).
17. Heaton, T.H. (1978) Generalized Ray Models of Strong Ground Motion, Ph.D. Thesis, California Institute of Technology, Pasadena, California.
18. Kanamori, H. (1979) A Semi-Empirical Approach to Prediction of Long-Period Ground Motions from Great Earthquakes, Bull. Seismol. Soc. Am., 69(No. 6):1645.

Table 4. Previous Investigations of Green's Functions Used to Synthesize Earthquakes

Investigator	Subject	Input to Model
Hartzell (1978)	Imperial Valley 1940	Aftershocks recorded at El Centro used as Green's functions
Heaton (1978, 1982)	San Fernando Feb. 9, 1971 (M=6.4)	P waves below 5 Hz with synthetics as Green's functions
Kanamori (1979)	Large historical earthquake (1857)	Used 1968 Borrego records as Green's functions
Hadley and HelMBERGER (1980)	Parkfield June 27, 1966 (M=5.7)	Aftershocks used as Green's functions
Irikura (1983)	1980 Izu-Hanto-Toho-Oki (M=6.7)	Delayed summation of small events
Wu (1983)	1982 Tangshan (M=5.3)	Aftershocks used as Green's functions (used accelerograms)
Hutchings (1985)	San Fernando (1971)	Small aftershocks (M<3.0)
Johnston (Present Study)	Theoretical M=7.5 for Wasatch Front, Utah	Magnitude 4-5 Earthquakes, time delayed

mountain records to predict or present a model of a record for the large historical earthquake that occurred pre-instrumentally. Hadley and HelMBERGER¹⁹ modeled the Parkfield earthquake using aftershocks. Irikura²⁰ used the delayed summation of small events to model the 1980 Izu-Manto-Toho-Oki event in Japan. Wu²¹ used accelerogram recordings of aftershocks to reproduce the 1982 Tangshan earthquake. Hutchings²² used small aftershocks (less than magnitude 3.0) to synthesize the 1971 San Fernando earthquake. Muramoto and Ohnuma²³ and Yoshikawa et al²⁴ have also elaborated on the

19. Hadley, D.M., and HelMBERGER, D.V. (1980) Simulation of Strong Ground Motion, Bull. Seismol. Soc. Am., 70(No. 2).
20. Irikura, K. (1983) Semi-Empirical Estimation of Strong Ground Motions During Large Earthquakes, Bull. Disas. Prev. Res. Inst., Kyoto Univ., 33(Part 2, No. 298):63.
21. Wu, F.T. (1983) A ground motion synthesis study using small earthquakes as Green's functions, Conference on Earthquake Hazards, Beijing, China.
22. Hutchings, L. (1985) Modeling Earthquakes with Empirical Green's Functions, Dept. of Geological and Environmental Studies, State Univ. of N.Y., Binghamton, N.Y.
23. Ohnuma, H., Muramatsu, I. (1985) Synthesis of strong ground motions by using the seismograms of aftershocks as Green's functions, Tokyo, Japan.
24. Yoshikawa, S., Kitano, T., Iwasaki, Y.T., and Tai, M. (1985) Prediction of strong ground motion by synthesis of small events records and site spectral ratio, Tokyo, Japan.

method. There have been several others who have successfully modeled moderate to large earthquakes using either foreshocks, aftershocks, or small, real or synthetic events from the area of the target large earthquake.

Modeling a future event gives rise to the same questions as modeling a past, pre-instrumental event. How is the validity of the result to be judged? There are various, obvious criteria for the addition of the seed events. Possibilities for the synthesis include the delayed addition of seed events, based on geometry (sum of seed rupture areas equals total fault area of target event), energy and moment. The synthesized waveforms will have new amplitudes and frequency content. If the amplitude were the only concern it could be raised by a simple scaling; however the spectrum of the composite event must also match that of the magnitude reasonably at both high and low frequencies. The basic assumption of this method is that the seismograms recorded at a distant site from small earthquakes truly approximate the response at the site to a unit impulse at the hypocenter, and therefore artificial incorporation of the effects of inhomogeneities along the ray path and attenuation with distance can be eliminated. However, the noise will be artificially accumulated: its effect must be compensated.

The approach this report takes toward the discrimination of a good synthesis of ground motion is to rely heavily on the previous conclusions of others who have successfully modeled a real event and to examine the consequences of the parameters chosen in our synthesis through the use of sensitivity tests of the data.

4. GREEN'S FUNCTION ADDITION OF SMALL EARTHQUAKES

4.1 Source Parameters Estimates and Conversions

After close examination of 15 events recorded at Golden, Colorado in the proper magnitude and distance range, five were used finally in the study. They had digitizable components, better signal versus noise and better reproduction of the record. Short period records at this range were especially difficult to digitize. The selected records are listed in Table 1. Their geographic locations and fault mechanisms, where available, are plotted on Figure 4, the numbers correspond to those on Table 1. The horizontal components have not been transformed into radial and transverse components since the actual epicenter station pair recording at Golden is to be modeled. Since many of the empirical relationships developed to relate fault and earthquake parameters

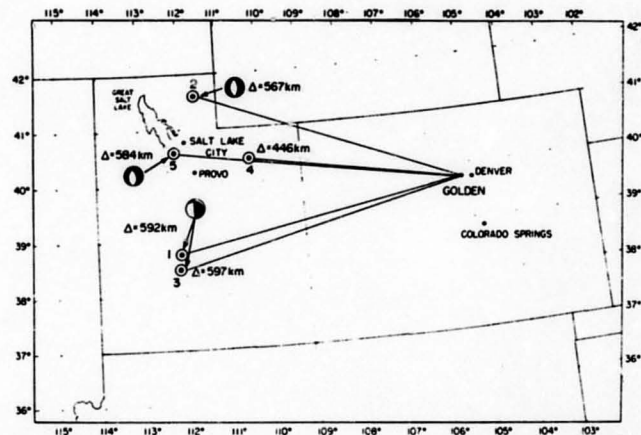


Figure 4. Location of Earthquakes Used in the Study. Single numbers refer to events in Table 1. Distances to Golden, Colorado, are listed in kilometers

to earthquake size utilize the surface wave magnitude scale (M_s) the observed magnitudes of the chosen events were converted to M_s . The empirically derived relationships of Nuttli²⁵ were used for this:

$$M_s = (m_b - 1.93)/0.61$$

$$M_s = (M_L - 2.28)/0.625$$

Energy estimates for several magnitudes are compiled in Table 5. The calculated values are derived from the relationship of Bath²⁶:

$$\log E = 1.44 M_s + 12.24$$

where E is the energy over the entire spectral range. Kanamori and Anderson²⁷ have verified that $E \sim 10^{1.5 M_s}$ from a theoretical examination of a simple dislocation model. The values of m_b , except when measured directly for the particular events, were converted by the equation of Brazee²⁸:

$$m_b = 1.276 + 0.749 M_L$$

because this conversion relation seemed consistent with this data set. One column of moments (M_0) are approximated from m_b using Nuttli's²⁹ average data for mid-plate earthquakes:

$$\log 10 M_0 = 2.0 m_b + 13.2$$

-
25. Nuttli, O.W. (1979) State-of-the-Art for Assessing Earthquake Hazards in the United States. Report 16. The Relation of Sustained Maximum Ground Acceleration and Velocity to Earthquake Intensity and Magnitude, Miscellaneous Paper S-73-1, U.S. Army Engineer Waterways Experiment Station.
 26. Bath, M. (1958) The energies of seismic body waves and surface waves. in Contributions in Geophysics: In Honor of Beno Gutenberg, Benioff, H., Ewing, M., Howell, Jr., B.F., and Press, F. Editors, Pergamon Press, New York, pp. 1-16.
 27. Kanamori, H., Anderson, D.L. (1975) "Theoretical Basis of Some Empirical Relationships in Seismology," Bull. Seismol. Soc. Am., 65(No. 5):1077-1095.
 28. Brazee, R.J. (1976) An Analysis of Earthquake Intensities With Respect to Attenuation, Magnitude and Rate of Recurrence, Final Report, NOAA Technical Memorandum EDS NGSDC-2.
 29. Nuttli, O.W. (1983) "Average Seismic Source-Parameter Relations for MID-Plate Earthquakes," Bull. Seismol. Soc. Am., 73(No. 2):519-535.

Table 5. Empirically Based Magnitude - Energy, Moment Pairs with Estimated Rupture

Event	M _b	M _L	M _S	Energy ⁺⁺	**M _o (Dyne-cm)	M _o ⁺	L (km)	W (km)	RUP AREA TOT (km ²)	\bar{D} (m)	**Assumed Depth (km)	Source Radius (km)
1	4.6*	4.0*	2.7	1.3 x 10 ¹⁶	2.5 x 10 ²²	4.5 x 10 ²²	2.0	2.0	4.0	.014	10	
2	4.8	4.6*	3.7	3.7 x 10 ¹⁷	6.3 x 10 ²²	8.1 x 10 ²³	3.0	3.0	9.0	.02	10	7.2
4	4.8*	4.7*	3.9	7.2 x 10 ¹⁷	6.3 x 10 ²²	4.3 x 10 ²³	3.0	3.0	9.0	.02	10	
3,5	5.1	5.2*	4.7	1 x 10 ¹⁹	2.5 x 10 ²³	2.5 x 10 ²⁴	4.0	4.0	16.0	.03	10	4.6
						4.0 x 10 ²³	3.1	3.1	9.6			
	6.5	7.0	7.5	1 x 10 ²³	1.6 x 10 ²⁶	7.1 x 10 ²⁵	20	13	269	1.1	10	
	6.9	7.5	8.3	1.6 x 10 ²⁴	1.0 x 10 ²⁷	2.1 x 10 ²⁶	40	20	800	3.7	10	

* Actual Observed for Event
 ** Nuttli Equation
 + Doser and Smith Equations
 ++ Bath 1958 Equation

15

BEST COPY AVAILABLE

The equations of Doser and Smith³⁰ for moments in the Utah area actually were used in calculations for the simulated composite events. The Wasatch Front earthquakes are not typical of the mid-plate regime, but lie somewhere between intra and interplate events in their characteristics (Nuttli²⁵, personal communication). Accordingly, size estimates for source dimensions were adjusted to fall between estimates of intra and interplate earthquakes (Table 5). Where studies have been performed on the specific events, these estimates are listed under "Source Radius".

Figure 5 shows the complete digitized records for events 1 through 5. The Fourier amplitude spectrum of each record was computed and is shown in Figure 6.

4.2 Geometric Approach

Initially the problem was approached from strictly geometric considerations. Estimates of the number of seeds and the dimensions of the cells were determined by a ratio of estimated rupture area of the seed events to that of the large earthquakes.

Figure 7 illustrates the concept. After a total fault rupture width and length are selected, the total area is divided up into cells of, in this report, equal area. In order to reduce the introduction of spurious periods from repetitive spacing the seed events are placed in random locations, one per cell. The location of the initial rupture is specified (generally at one end) and the earthquake seed recordings are stacked with delays corresponding to distance from the initial rupture cell denuded by the rupture velocity (see Figure 8). This computational procedure was followed for all the models, only the number of cells and consequently the number of seeds as well as the cell dimensions are changed.

The resulting composite earthquakes from this stacking had unsatisfactorily small amplitudes and energies of the modeled event, however, several valuable sensitivity tests were performed with this initial model.

4.2.1 RUPTURE VELOCITY SENSITIVITY

To demonstrate the effect of assumed rupture velocity on the composite event, the Z components of events number 3 and 5 were used. In Figure 9a and b, the first record is the actual recording of the seed earthquake, the next 3 records are the result of delayed summation of 67 seed events at rupture velocities of 2.0 km/sec, 2.5 km/sec and 1.7 km/sec in sequence. The last records in a and b are for a stacking of 2.0 km/sec but with double the original number of seed events. In all cases the total fault area modelled was 45 km by 29 km. Inspection of Figure 9 reveals what would generally be expected: as the velocity of rupture increases less of the high frequency character of the original waveform is preserved. Also, holding the rupture velocity and the

30. Doser, D.I., and Smith, R.B. (1982) "Seismic Moment Rates in the Utah Region," Bull. Seismol. Soc. Am., 72(No. 2):525-551.

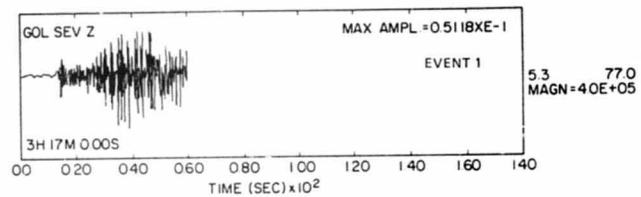


Figure 5a. Digitized Records of Seed Earthquakes Used to Create Composite Earthquakes for a Short Period

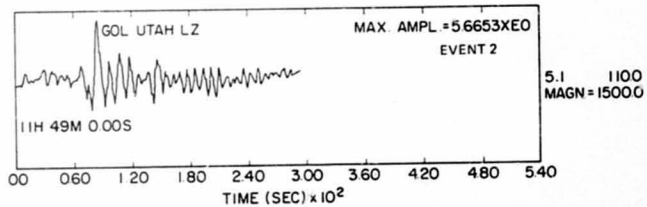


Figure 5b. Digitized Records of Seed Earthquakes Used to Create Composite Earthquakes for a Long Period

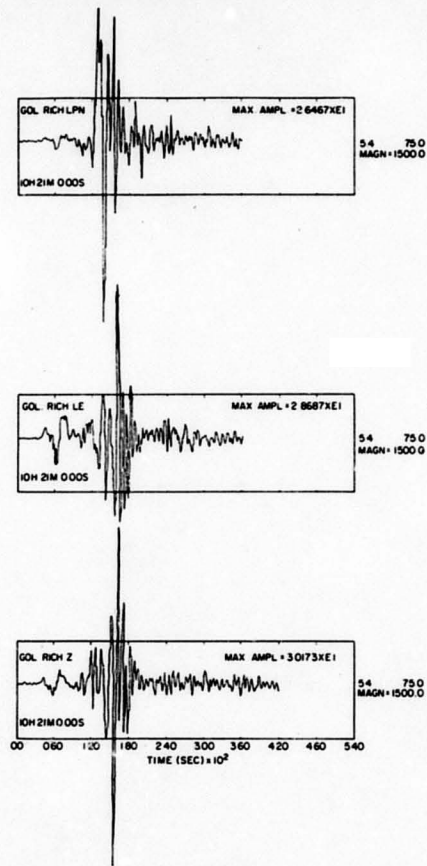


Figure 5c. Digitized Records of Seed Earthquakes Used to Create Composite Earthquakes for a Long Period (2.5 vert exaggeration)

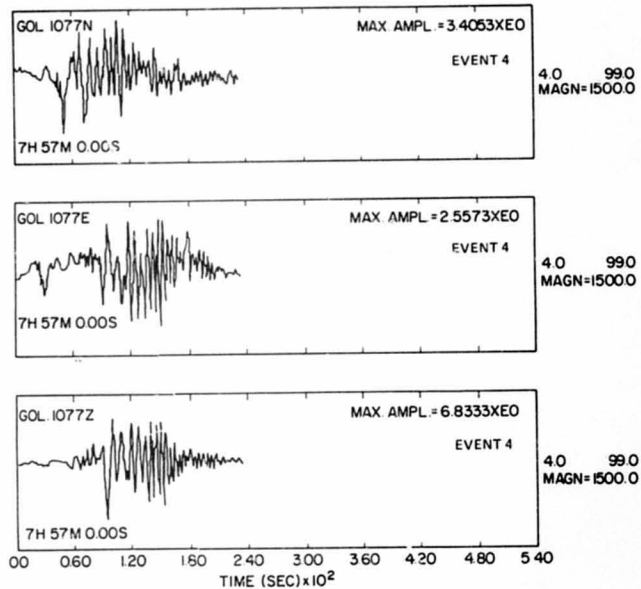


Figure 5d. Digitized Records of Seed Earthquakes Used to Create Composite Earthquakes for a Long Period

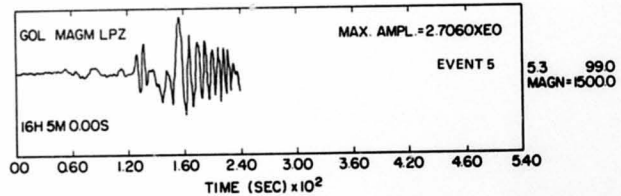


Figure 5e. Digitized Records of Seed Earthquakes Used to Create Composite Earthquakes for a Long Period

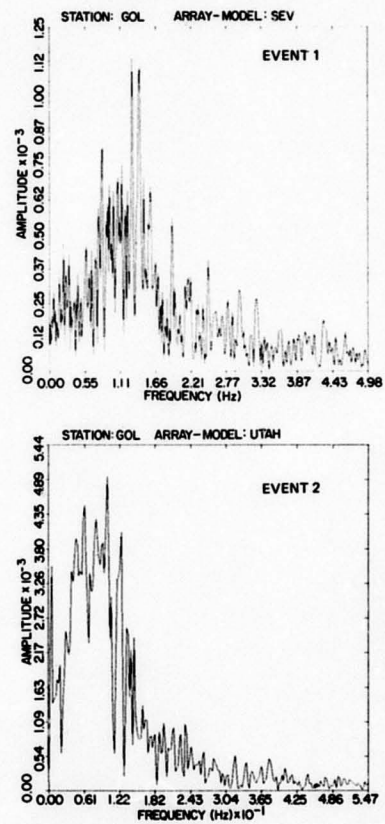


Figure 6. Spectra of Seed Earthquakes as Recorded at Golden WWSSN (a) Event 1; (b) Event 2

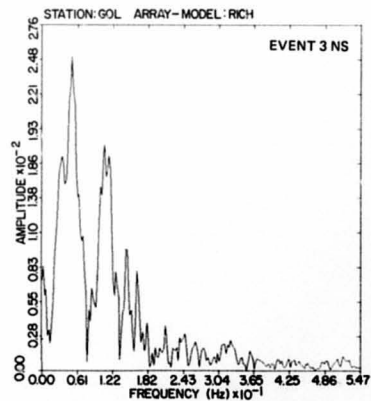
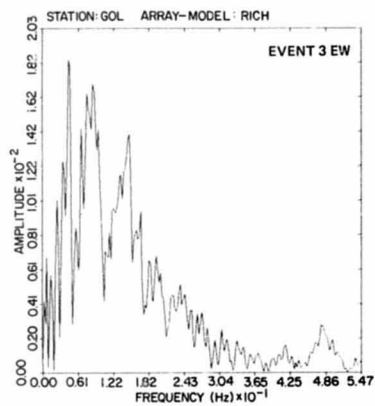


Figure 6c. Spectra of Seed Earthquakes as Recorded at Golden WWSSN

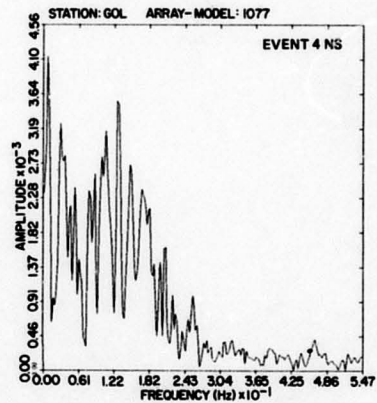
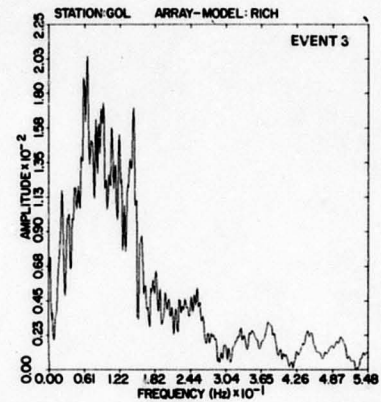


Figure 6. Spectra of Seed Earthquakes as Recorded at Golden WWSSN, (c) Event 3; (d) Event 4

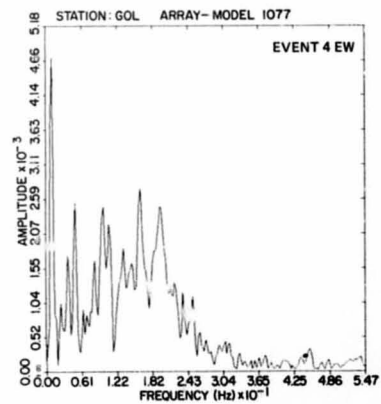
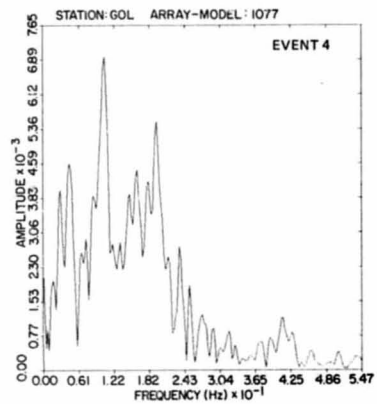


Figure 6d. Spectra of Seed Earthquakes as Recorded at Golden WWSSN

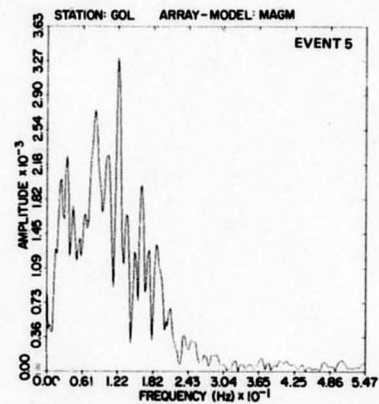


Figure 6e. Spectra of Seed Earthquakes as Recorded at Golden WWSSN

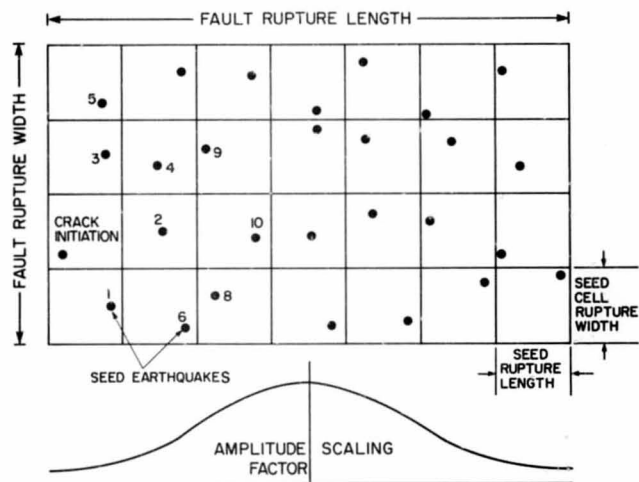
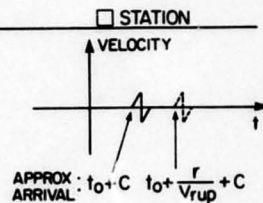
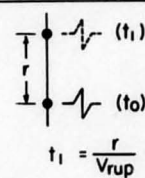
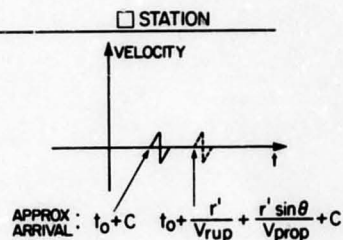
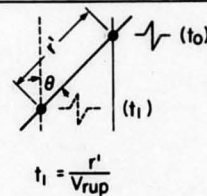


Figure 7. Model of Earthquake Rupture Process. After crack initiation, cells rupture in order of closest distances. Amplitude scaling is optional

a) VERTICAL FAULT (SIDE VIEW)



b) DIPPING FAULT (SIDE VIEW)



r, r' = Distance from initial rupture seed to next closest seed rupture.
 V_{rup} = Rupture velocity along the fault.
 V_{prop} = Velocity of propagation along the path to the station.

Figure 8. a) Vertical Fault Model, b) Dipping Fault Model

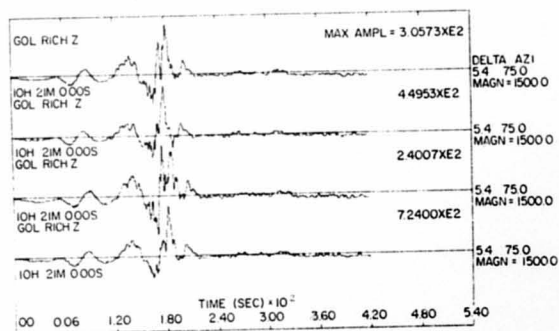
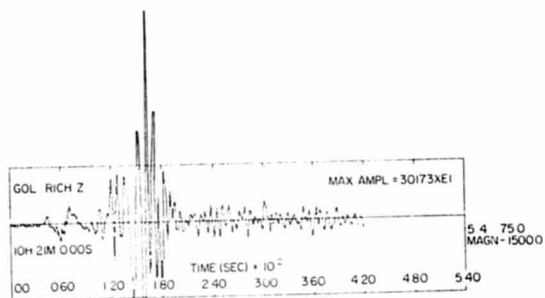


Figure 9a. Original Record, $V_{rup} = 2.0$ km/sec, 2.5 km/sec, 1.7 km/sec. (2.5 vert exaggeration) and $V_{rup} = 2.0$ km/sec with Number of Seed Events = 134 for Event 3. Cracking starts at edge of fault

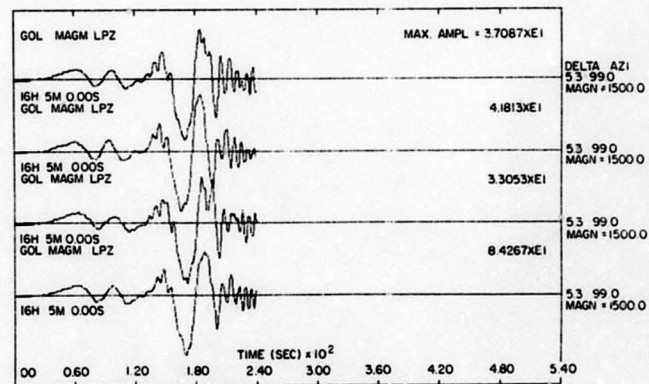
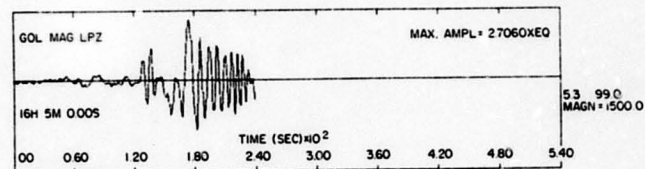


Figure 9b. Original Record, $V_{rup} = 2.0$ km/sec, 2.5 km/sec, 1.7 km/sec, and $V_{rup} = 2.0$ km/sec with Number of Seed Events = 134 for Event 5. Cracking starts at edge of fault

composite fault dimensions constant but doubling the number of seed events, as in the bottom record, has the effect of washing out the high frequencies while doubling the maximum amplitude. Figure 9b, one of the most dramatic shifts to longer periods for this model demonstrates the effect of what is in effect a convolution with a longer source time function. Note that again the greatest high frequency content appears in the 4th waveform, that with the slowest rupture. The first 2 records of Figure 9b appear again in Figure 10 along with the fast fourier spectra of the entire waveforms. This stacking shifts the maximum period from approximately 8 seconds up to 33 seconds. The spectrum dips dramatically at a frequency corresponding to the period it takes for the rupture to propagate from one end of the fault to the other.

4.2.2 INITIAL CRACKING POSITION

The predominant long period peak produced in Figure 9b and 10 was examined more closely. As seen from Figure 9b, it is not sensitive to reasonable changes in rupture velocity nor to a factor of 2 change in the number of seed events. Figure 11a and 11b show the 2.0 km/sec rupture model with crack initiation at the center for the Richfield (a) and Magna (b) earthquakes.

At this distance, starting the crack at the center of the fault, rather than at one side, can be compared to having a fault one half the length with the cell number held constant. The resulting waveforms are different but similar in frequency content; the effect on the amplitude is to raise it as if doubling the number of seed events.

4.2.3 NOISE ACCUMULATION

This algorithm for stacking seed earthquake recordings also stacks the noise in the record. In the examples Section 4.2.1, 4.2.2 above, the noise during the minutes previous to the onset of the event was digitized. These were then stacked according to the same geometry as the composite earthquake. For these sensitivity tests the contribution was an order of magnitude smaller than the resulting signal so the noise was ignored. This assumes that the noise was more or less constant from the time prior to the arrival into the first few minutes of the seed event. In later runs (Section 4.3 below, where larger numbers of seeds were added), the noise accumulation effects were corrected by either 1) filtering the noise from the seed events before stacking or 2) filtering the composite event recording.

4.3 Energy and Moment Approach

The geometric approach (Section 4.2) from energy considerations alone clearly leads to underestimates in the number of seed events. This is probably because the total rupture area that might be associated with an earthquake is larger than the cell size associated with an echelon rupture.

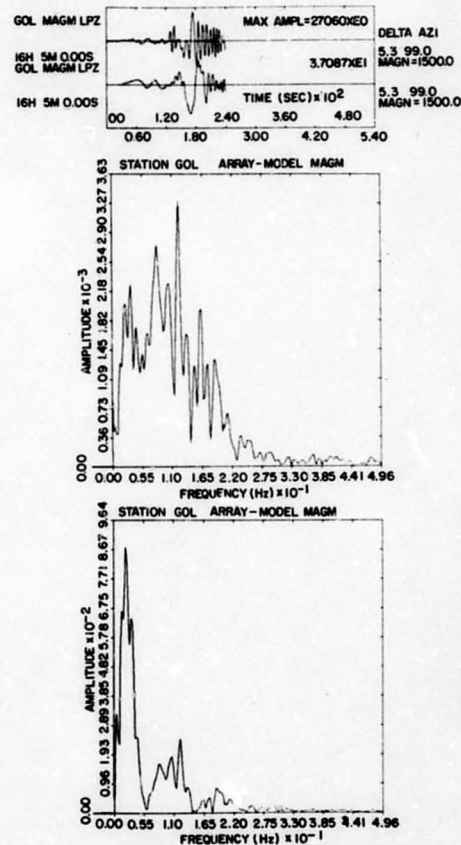


Figure 10. Magna Earthquake Records and Spectra Before Stacking and After (Model: 45 km x 29 km, $V_{rup} = 2.0$ km/sec, NS = 67). Cracking starts at edge of fault

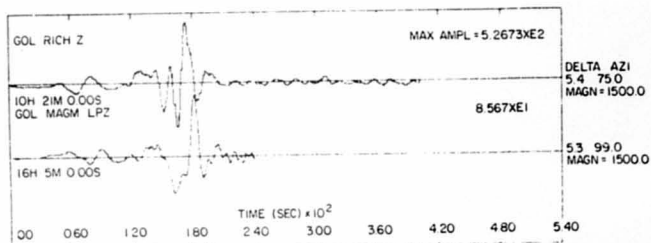


Figure 11. Effect of Central Crack Initiation: a) Event 3, Z Component; and b) Event 5, Z Component

For seismic hazard purposes, often more important than the absolute level of ground motion is the frequency at which it occurs. For this reason, the final composite events were synthesized according to the criteria of Joyner and Boore¹⁵. Their analysis showed that, as in the present case where the recording distances are large compared to the source dimensions, the spectrum of the composite event can be made to conform at both high and low frequencies to the ω -squared fault rupture model with constant $M_o f_o^{-3}$ scaling (M_o = composite moment, f_o = corner frequency).

Their criterion for the random summation is as follows:

$$\eta = (M_o / M_{oe})^{1/3}$$

$$\kappa = (M_o / M_{oe})^{-1/3}$$

where M_{oe} is the seed event moment; η is the number of seed events to be summed; κ is a scaling factor. Table 6 lists these values for the trial seed events 1 through 5 for a target event of moment = 2.1×10^{26} dyne-cm for a total fault area of 900 km^2 ($45 \text{ km} \times 20 \text{ km}$).

Figure 12 shows the resulting waveforms. Note the very prominent long periodicity of the resulting waveform. Figure 13 presents the spectra. The spectrum of the noise previous to event number one was analyzed and filtered out of the record. (the noise is artificially accumulated with the composite methodology). A high pass filter cutoff of 0.25 Hz was applied to event 1 shown in Figure 12a and a cutoff of .025 Hz was applied to event 4's waveform. Event 4 is shown after filtering in Figure 12.

Table 6. Composite Parameters for Waveforms in Figure 12

Event	Component	η	Suggested Scale Factor (κ)	Cell Dimensions (km)	AMP (Composite) / AMP (Seed)
1	SZ	170,241	0.049	0.072	10^3
2	LZ	1,650	0.157	0.738	10^3
3	LNS	367	0.229	1.566	10^2
	LEW				10^1
	LZ				10^2
4	LNS	3,838	0.127	0.484	10^3
	LEW				10^3
	LZ				10^3
5	LZ	4,226	0.124	0.461	10^3

Tabulated in Table 6 are the ratios of original peak amplitude from the digitized portion of the seed record to that of the resulting composite. They are in the range of $10^{-2} - 10^{-3}$ which is what would be expected for the larger target magnitude. Since the seed earthquakes are all in the magnitude range of 4 to 5, they really are too large to be considered as having the full high frequency content of the true impulse response, however, with this station's sensitivity smaller events are not well-recorded at this distance range.

4.3.1 INCOHERENT RUPTURE

Extensive sensitivity tests of barrier effects were not run because of the hypothetical nature of a future event. Figure 14 does show the results of breaking the fault into two pieces, with less than a half kilometer separation. Figure 14a is the coherent fault rupture for comparison purposes and Figure 14b is the "broken" rupture. The difference in this case is minimal. Further discussion of this topic can be found in Section 5.

5. DISCUSSION

There was some success modeling at least arrival times for some of the seed events with conventional synthetics. The best match of the initial arrivals for a few test cases used a trapezoidal time function of 1.5 to 2 second's duration. At earth structure of

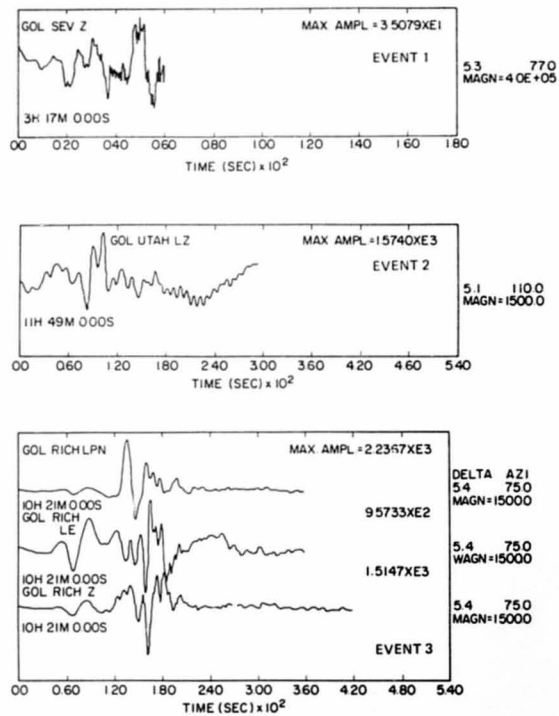


Figure 12. Composite Earthquakes from Wasatch Front as Predicted to be Measured at Gol. Short period record event number 1 high-pass filtered at 0.25 Hz. Long period record event number 4 high-pass filtered at 0.025 Hz. (a) Event 1; (b) Event 2; (c) Event 3

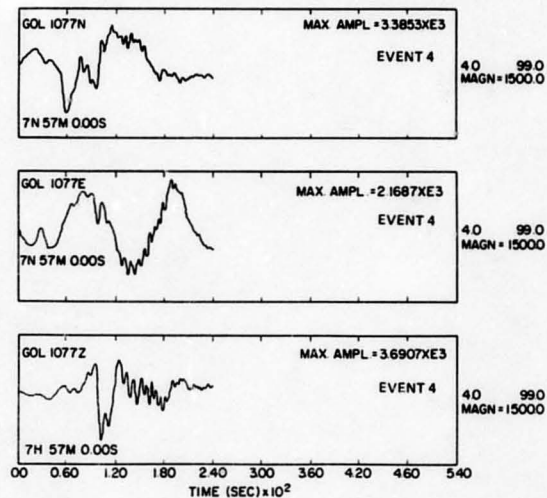


Figure 13d. Composite Earthquakes from Wasatch Front as Predicted to be Measured at Gol. Short period record event number 1 high-pass filtered at 0.25 Hz. Long period record event number 4 high-pass filtered at 0.025 Hz

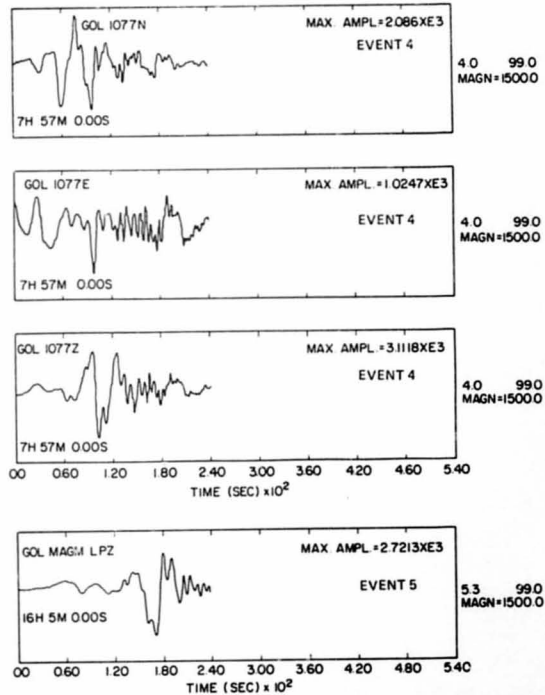


Figure 12. Composite Earthquakes from Wasatch Front as Predicted to be Measured at Gol. Short period record event number 1 high-pass filtered at 0.25 Hz. Long period record event number 4 high-pass filtered at 0.025 Hz; (12d cont) Event 4; (12e) Event 5

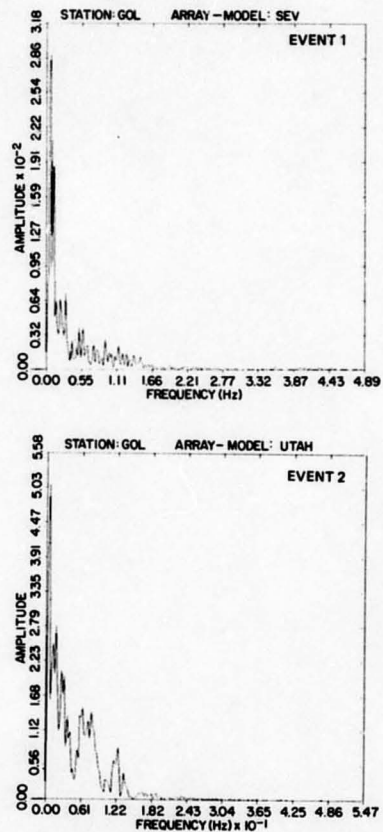


Figure 13. Spectra of Composite Events. Events 1 and 4 have been filtered to remove noise; (a) Event 1; (b) Event 2

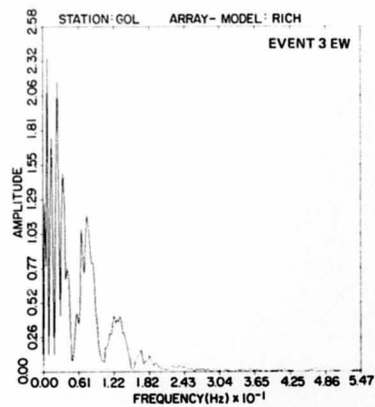
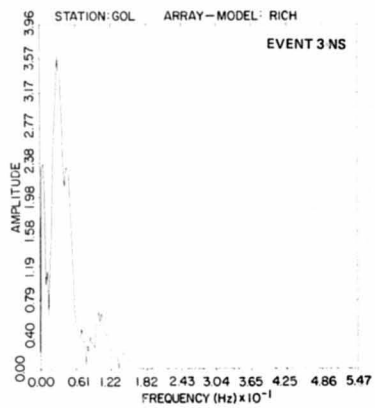


Figure 13c. Spectra of Composite Events. Events 1 and 4 have been filtered to remove noise

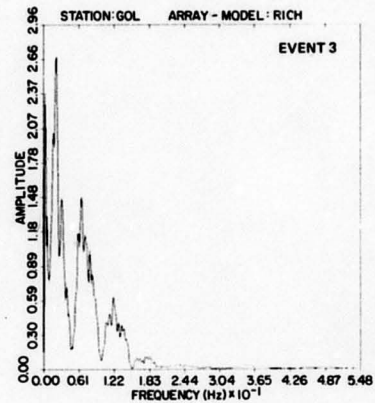


Figure 13c (cont). Spectra of Composite Events. Events 1 and 4 have been filtered to remove noise

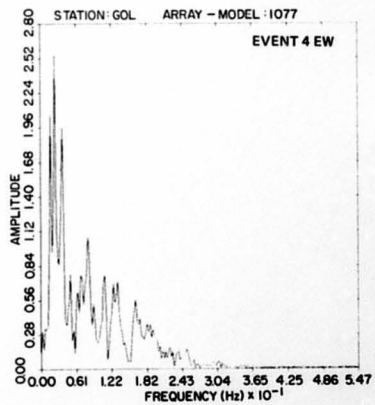
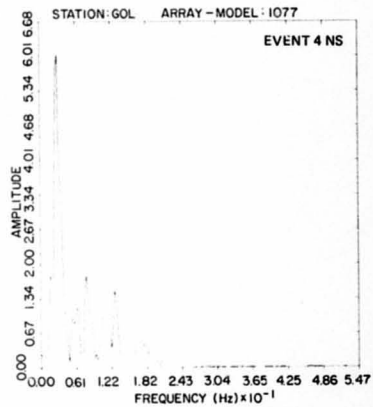


Figure 13d. Spectra of Composite Events. Events 1 and 4 have been filtered to remove noise

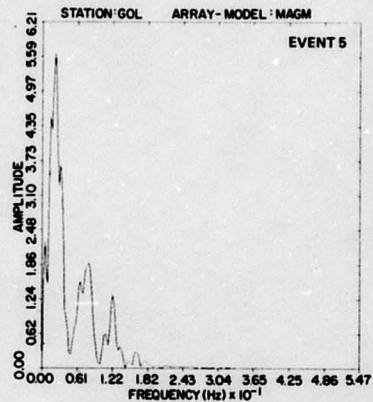
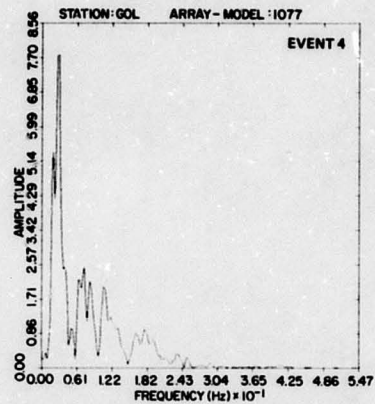


Figure 13. Spectra of Composite Events. Events 1 and 4 have been filtered to remove noise; (d) (cont) Event 4; (e) Event 5

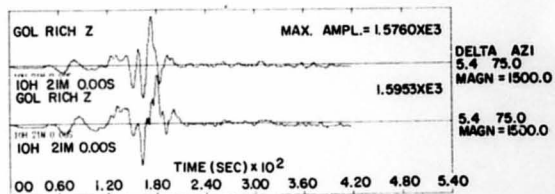


Figure 14. a) Event 3 Normal Composite Earthquake
 b) Event 3 Composite Earthquake with
 Central Barrier on Fault

P.S. ρ , $h = 6.2$ km/sec, 3.6 km/sec, 2.7 g/cm³, 2.5 km; 6.8 km/sec, 3.9 km/sec, 2.8 g/cm³, 15 km over a 7.8 km/sec, 4.5 km/sec halfspace was used ($h =$ thickness). However, several extensive studies^{31,32} have examined waveforms recorded at Golden for similar although longer paths. Helmburger and Engen³¹ found that long period waveforms were insensitive to crustal variations to the point where a simple layer over a halfspace model would suffice. They used a P-velocity, S-velocity and density of 6.2 km/sec, 3.5 km/sec and 2.7 g/cc respectively with a thickness of 32 km, over an 8.2 km/sec, 4.5 km/sec, 3.4 g/sec halfspace. Figure 15a shows their analysis of arrivals for the long period, east-west record at Golden from an earthquake in California. In Figure 15b, a long period, east-west record from the current data base is shown for comparison purposes. Note the similarity of the arrivals (P_n , P_L , Rayleigh) in the Richfield event (Figure 15b) to those in Figure 15a.

In none of the calculated composite events has more than one recording been used repeatedly. If the event is conjectured to involve several faults, on which small earthquakes have occurred, then, for example, one third of the modeled fault could use sequential addition of one recording, the middle could use another and the last third yet another, as in some of the aftershock composites studies (Section 3.).

This study was undertaken to examine the feasibility of using the method as a test case. If the high frequency content of the ground motion is of interest, the range of usefulness of the method is limited in this area. The high frequencies are suppressed for two reasons: 1) the high frequency component of the composite event is controlled by the spectra of the seed events. To in fact be a legitimate impulse response, smaller seed events must be used ($M < 3.5$), and 2) the calculation of the composite event permits the low frequencies to add coherently and the high frequencies to add incoherently.

The first reason is a practical constraint caused by the need for clear, digitizable, broad-band waveforms at the large distance range. The second is a real effect of the physical rupture process.

6. CONCLUSIONS

Construction of a composite earthquake as in this report eliminates the need for detailed understanding of the crustal structure. The effects of inhomogeneities along the ray path have been automatically incorporated into the resulting waveforms. The validity of this method has been proven by other investigators. Excluded in the present

31. Helmburger, D.V., and Engen, G.R. (1980) Modeling the Long-Period Body Waves from Shallow Earthquakes at Regional Distances, *Bull. Seismol. Soc. Am.*, 70(No. 5):1699-1714.
32. Wallace, T.C., Helmburger, D.V., and Melman, G.R. (1981) A Technique for the Inversion of Regional Data is Source Parameter Studies, *J. Geophys. Res.*, 86(No. B3):1679-1685.

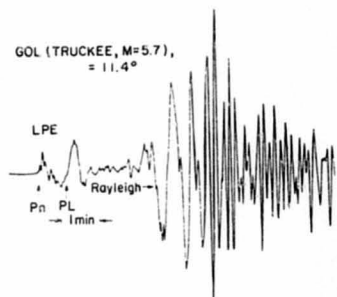


Figure 15a. Two Recordings at Golden WSSN, Truckee Earthquake Arrivals (as analyzed by HelMBERGER and ENGEN, 1980)

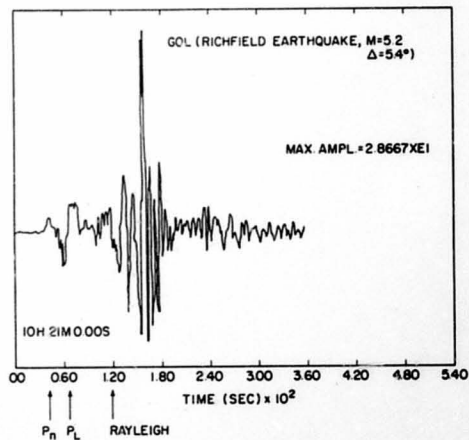


Figure 15b. Two Recordings at Golden WSSN, Richfield Earthquake (this study)

analysis are the effects of incoherent rupture (other than Figure 14), irregular major asperities or starting and stopping phases. The extent to which irregularities in the rupture process might occur during a large event for the Wasatch area is at present unpredictable. However, sensitivity tests can be conducted with various artificial rupture barrier models and it is useful to do so. Such conditions have been known to cause high frequency spikes in the ground motion of large earthquakes. In this analysis the effects of small scale asperities have been included by the incorporation of random positioning of seed events within the cells. The resulting waveforms have been shown to be insensitive to realistic variations in rupture velocity, and to small changes in rupture initiation position.

The waveforms prescribed in Section 4.3, although somewhat deficient in high frequency, can be used to model ground motion from a large ($M \sim 7.5$) earthquakes from the exact seed locations to be recorded at the site of the Golden, Colorado WSSN instrument.

NOTE: T. Heaton³³ (personal communication, 1985) found the suitable moment ratio for summation to be tentatively $M_o/M_{oe} = 2/3$ where M_o is the composite moment and M_{oe} is the seed moment. He based his preliminary conclusion on a synthesis of the Chilean (1960) earthquake ground motion with a Western US site seed event. His constraint was the matching of the teleseismic records to that of the composite and he used larger sized seeds ($M \sim 6$ to 8) since it was necessary to use large ranges.

33. Heaton, T. (1985) "Strong motion estimates for Hypothetical Earthquakes on the Cascadia Subduction Zone," paper presented at AGU meeting, Dec 9-13, 1985, San Francisco, California.

References

1. Smith, R.B. (1975) "Seismicity and Earthquake Hazards of the Wasatch Front, Utah," Hearing before the Committee on Aeronautical and Space Sciences, United States Senate, 94th Congress, U.S. Government Printing Office, Washington, D.C.
2. Battis, J.C. (1982) "Seismic Hazard Study for Utah," AFGL-TR-82-0319, ADA129238.
3. Hamilton, W., and Myers, W.B. (1966) Cenozoic Tectonics of the Western United States, Reviews of Geophysics, 4(No. 4):509-549.
4. Priestley, K., and Brune, J. (1978) Surface Waves and the Structure of the Great Basin of Nevada and Western Utah, J. Geophys. Res., 83(No. B5):2265-2272.
5. Bucher, R.L., and Smith, R.B. (1971) Crustal Structure of the Eastern Basin and Range Province and the Northern Colorado Plateau from Phase Velocities of Rayleigh Waves, in The Structure and Physical Properties of the Earth's Crust, John G. Heacock, ed., Geophysical Monograph 14, AGU, Washington, D.C.
6. Keller, G.R., Braille, L.W., and Morgan, P. (1979) Crustal Structure, Geophysical Models and Contemporary Tectonism of the Colorado Plateau, Tectonophysics, 61:131-147.
7. Thompson, G.A., Zoback, M.L. (1979) Regional Geophysics of the Colorado Plateau, Tectonophysics, 61(No. 1-3):149-181.
8. Keller, G.R., Smith, R.B., and Braille, L.W. (1975) Crustal Structure Along the Great Basin - Colorado Plateau Transition from Seismic Refraction Studies, J. Geophys. Res., 80(No. 8):1093-1098.
9. Jackson, W.H., and Pakiser, L.C. (1965) Seismic Study of Crustal Structure in the Southern Rocky Mountains, U.S. Geological Survey Prof. Paper 525D, pp. D85-D92.
10. Prodehl, C., and Pakiser, L.C. (1980) Crustal Structure of the Southern Rocky Mountains from Seismic Measurements, Bull. Seismol. Soc. Am., 91:147-155.
11. Archambeau, C.B., Flinn, E.A., and Lambert, D.G. (1969) Fine Structure of the Upper Mantle, J. Geophys. Res., 74(No. 25):5825-5865.
12. Burdick, L.J. (1977) Broad-Band Seismic Studies of Body Waves, Ph.D. Thesis, California Institute of Technology.
13. Biswas, N.N., and Knopoff, L. (1974) The Structure of the Upper Mantle under the United States from the Dispersion of Rayleigh Waves, GJRRAS, 36(No. 3):515-539.
14. Aki, K., and Richards, P.G. (1979) Quantitative Seismology, Theory and Methods, Vol. 1, W.H. Freeman and Co., San Francisco, California.
15. Joyner, W.B. and Boore, D.M. (1985) "On Simulating Large Earthquakes by Green's Function Addition of Smaller Earthquakes," manuscript submitted to the Proceedings of the 5th Maurice Ewing Symposium - Earthquake Source Mechanics, May 19-23, (1985) Harriman, N.Y.
16. Hartzel, S.H. (1978) Earthquake Aftershocks as Green's Functions, Geophys. Res. Letts, 5(No. 1).
17. Henton, T.H. (1978) Generalized Ray Models of Strong Ground Motion, Ph.D. Thesis, California Institute of Technology, Pasadena, California.
18. Kanamori, H. (1979) A Semi-Empirical Approach to Prediction of Long-Period Ground Motions from Great Earthquakes, Bull. Seismol. Soc. Am., 69(No. 6):1645.
19. Hadley, D.M., and HelMBERGER, D.V. (1980) Simulation of Strong Ground Motion, Bull. Seismol. Soc. Am., 70(No. 2).
20. Irikura, K. (1983) Semi-Empirical Estimation of Strong Ground Motions During Large Earthquakes, Bull. Dias. Prev. Res. Inst., Kyoto Univ., 33(Part 2, No. 298):63.
21. Wu, F.T. (1983) A ground motion synthesis study using small earthquakes as Green's functions, Conference on Earthquake Hazards, Beijing, China.
22. Hutchings, L. (1985) Modeling Earthquakes with Empirical Green's Functions, Dept. of Geological and Environmental Studies, State Univ. of N.Y., Binghamton, N.Y.
23. Ohnuma, H., Muramatsu, I. (1985) Synthesis of strong ground motions by using the seismograms of aftershocks as Green's functions, Tokyo, Japan.
24. Yoshikawa, S., Kitano, T., Iwasaki, Y.T., and Tai, M. (1985) Prediction of strong ground motion by synthesis of small events records and site spectral ratio, Tokyo, Japan.
25. Nuttli, O.W. (1979) State-of-the-Art for Assessing Earthquake Hazards in the United States, Report 16, The Relation of Sustained Maximum Ground Acceleration and Velocity to Earthquake Intensity and Magnitude, Miscellaneous Paper S-73-1, U.S. Army Engineer Waterways Experiment Station.
26. Bath, M. (1958) The energies of seismic body waves and surface waves, in Contributions in Geophysics: In Honor of Gutenberg, Beno, Benioff, H., Ewing, M., Howell, Jr., B.F., and Press, F. Editors, Pergamon Press, New York, pp. 1-16.
27. Kanamori, H., Anderson, D.L. (1975) "Theoretical Basis of Some Empirical Relationships in Seismology," Bull. Seismol. Soc. Am., 65(No. 5):1077-1095.
28. Brazee, R.J. (1976) An Analysis of Earthquake Intensities With Respect to Attenuation, Magnitude and Rate of Recurrence, Final Report, NOAA Technical Memorandum EDS NGSDC-2.
29. Nuttli, O.W. (1983) "Average Seismic Source-Parameter Relations for MID-Plate Earthquakes," Bull. Seismol. Soc. Am., 73(No. 2):519-535.

30. Doser, D.J., and Smith, R.B. (1982) "Seismic Moment Rates in the Utah Region," Bull. Seismol. Soc. Am., 72(No. 2):525-551.
31. Helmberger, D.V., and Engen, G.R. (1980) Modeling the Long-Period Body Waves from Shallow Earthquakes at Regional Distances, Bull. Seismol. Soc. Am., 70(No. 5):1699-1714.
32. Wallace, T.C., Helmberger, D.V., and Mellman, G.R. (1981) A Technique for the Inversion of Regional Data in Source Parameter Studies, J. Geophys. Res., 86(No. B3):1673-1685.
33. Heaton, T. (1985) "Strong motion estimates for Hypothetical Earthquakes on the Cascadia Subduction Zone," paper presented at AGU meeting, Dec 9-13, 1985, San Francisco, California.

Bibliography

- Aki, K., and Richards, P.G. (1979) Quantitative Seismology. Theory and Methods, Vol. I, W.H. Freeman and Co., San Francisco, California.
- Archambeau, C.B., Flinn, E.A., and Lambert, D.G. (1969) Fine Structure of the Upper Mantle, J. Geophys. Res., 74(No. 25):5825-5865.
- Bache, T.C., Rodi, W.L., and Harkrider, D.G. (1978) Crustal Structures Inferred from Rayleigh-Wave Signatures of NTS Explosions, Bull. Seismol. Soc. Am., 68(No. 5):1399-1413.
- Bath, M. (1958) The energies of seismic body waves and surface waves, in Contributions in Geophysics: In Honor of Beno Gutenberg, Benioff, H., Ewing, M., Howell, Jr., B.F., and Press, F. Editors, Pergamon Press, New York, pp. 1-16.
- Battis, J.C., (1982) "Seismic Hazard Study for Utah," AFGL-TR-82-0319, ADA129238.
- Berg, J.W., Cook, K.L., Narans, H.D., and Dolan, W.M. (1960) Seismic Investigation of Crustal Structure in the Eastern Part of the Basin and Range Province, Bull. Seismol. Soc. Am., 50(No. 4):511-535.
- Biswas, N.N., and Knopoff, L. (1974) The Structure of the Upper Mantle under the United States from the Dispersion of Rayleigh Waves, GJRAS, 36(No. 3):515-539.
- Braille, L.W., Smith, R.B., Keller, G.R., Welch, R.M., and Meyer, R.P. (1974) Crustal Structure Across the Wasatch Front from Detailed Seismic Refraction Studies, J. Geophys. Res., 79(No. 17):2669-2677.
- Braze, R.J. (1976) An Analysis of Earthquake Intensities With Respect to Attenuation, Magnitude and Rate of Recurrence, Final Report, NOAA Technical Memorandum EDS NGSDC-2.
- Bocher, R.L., and Smith, R.B. (1971) Crustal Structure of the Eastern Basin and Range Province and the Northern Colorado Plateau from Phase Velocities of Rayleigh Waves, in The Structure and Physical Properties of the Earth's Crust, John G. Heacock, ed., Geophysical Monograph 14, AGU, Washington, D.C.
- Burdick, L.J. (1977) Broad-Band Seismic Studies of Body Waves, Ph.D. Thesis, California Institute of Technology.

- Cheng, Chiung-Chuan, and Mitchell, B.J. (1981) Crustal Q Structure in the United States from Multi-Mode Surface Waves, Bull. Seismol. Soc. Am., 71(No. 1):161-181.
- Doser, D.I., and Smith, R.B. (1982) "Seismic Moment Rates in the Utah Region," Bull. Seismol. Soc. Am., 72(No. 2):525-551.
- Hadley, D.M., and Heimberger, D.V. (1980) Simulation of Strong Ground Motion, Bull. Seismol. Soc. Am., 70(No. 2).
- Hamilton, W., and Myers, W.B. (1966) Cenozoic Tectonics of the Western United States, Reviews of Geophysics, 4(No. 4):509-549.
- Hartzel, S.H. (1978) Earthquake Aftershocks as Green's Functions, Geophys. Res. Letts., 5(No. 1).
- Heaton, T.H. (1978) Generalized Ray Models of Strong Ground Motion, Ph.D. Thesis, California Institute of Technology, Pasadena, California.
- Heaton, T.H. (1982) The 1972 San Fernando Earthquake: A Double Event? Bull. Seismol. Soc. Am., 72(No. 6).
- Heaton, T. (1985) "Strong motion estimates for Hypothetical Earthquakes on the Cascadia Subduction Zone," paper presented at AGU meeting, Dec 9-13, 1985, San Francisco, California.
- Heimberger, D.V., and Engen, G.R. (1980) Modeling the Long-Period Body Waves from Shallow Earthquakes at Regional Distances, Bull. Seismol. Soc. Am., 70(No. 5):1699-1714.
- Hill, D.P., and Pakiser, L.C. (1967) Seismic-Refraction Study of Crustal Structure between the Nevada Test Site and Boise, Idaho, Bull. Geol. Soc. Am., 78(No. 6):685-704.
- Hutchings, L. (1985) Modeling Earthquakes with Empirical Green's Functions, Dept. of Geological and Environmental Studies, State Univ. of N.Y., Binghamton, N.Y.
- Irikura, K. (1983) Semi-Empirical Estimation of Strong Ground Motions During Large Earthquakes, Bull. Disas. Prev. Res. Inst., Kyoto Univ., 33(Part 2, No. 298):63.
- Jackson, W.H., Stewart, S.W., and Pakiser, L.C. (1963) Crustal Structure in Eastern Colorado from Seismic Refraction Measurements, J. Geophys. Res., 68:5767-5776.
- Jackson, W.H., and Pakiser, L.C. (1965) Seismic Study of Crustal Structure in the Southern Rocky Mountains, U.S. Geological Survey Prof. Paper 525D, pp. D85-D92.
- Joyner, W.B. and Boore, D.M. (1985) "On Simulating Large Earthquakes by Green's Function Addition of Smaller Earthquakes," manuscript submitted to the Proceedings of the 5th Maurice Ewing Symposium - Earthquake Source Mechanics, May 19-23, (1985) Harriman, N.Y.
- Kanamori, H., Anderson, D.L. (1975) "Theoretical Basis of Some Empirical Relationships in Seismology," Bull. Seismol. Soc. Am., 65(No. 5):1077-1095.
- Kanamori, H. (1979) A Semi-Empirical Approach to Prediction of Long-Period Ground Motions from Great Earthquakes, Bull. Seismol. Soc. Am., 69(No. 6):1645.
- Keller, G.R., Smith, R.B., and Braille, L.W. (1975) Crustal Structure Along the Great Basin - Colorado Plateau Transition from Seismic Refraction Studies, J. Geophys. Res., 80(No. 8):1093-1098.
- Keller, G.R., Smith, R.B., Braille, L.W., Heavey, R., and Shurbet, D.H. (1976) Upper Crustal Structure of the Eastern Basin and Range, Northern Colorado Plateau, and Middle Rocky Mountains from Rayleigh Wave Dispersion, Bull. Seismol. Soc. Am., 66(No. 3):869-876.

- Keller, G.R., Braile, L.W., and Morgan, P. (1979) Crustal Structure, Geophysical Models and Contemporary Tectonism of the Colorado Plateau, Tectonophysics, 61:131-147.
- Nuttli, O.W. (1983) "Average Seismic Source-Parameter Relations for MID-Plate Earthquakes," Bull. Seismol. Soc. Am., 73(No. 2):519-535.
- Nuttli, O.W. (1979) State-of-the-Art for Assessing Earthquake Hazards in the United States. Report 16, The Relation of Sustained Maximum Ground Acceleration and Velocity to Earthquake Intensity and Magnitude. Miscellaneous Paper S-73-1, U.S. Army Engineer Waterways Experiment Station.
- Ohnuma, H., Muramatsu, I. (1985) Synthesis of strong ground motions by using the seismograms of aftershocks as Green's functions, Tokyo, Japan.
- Priestley, K., and Brune, J. (1978) Surface Waves and the Structure of the Great Basin of Nevada and Western Utah, J. Geophys. Res., 83(No. B5):2265-2272.
- Prodehl, C., and Pakiser, L.C. (1980) Crustal Structure of the Southern Rocky Mountains from Seismic Measurements, Bull. Seismol. Soc. Am., 91:147-155.
- Roller, J.C. (1965) Crustal Structure in the Eastern Colorado Plateaus Province from Seismic-Refraction Measurements, Bull. Seismol. Soc. Am., 55(No. 1):107-119.
- Slemmons, D.B. (1977) "Faults and Earthquake Magnitude," State-of-the-Art for Assessing Earthquake Hazards in the United States, Report 6, Misc. paper S-73-1, U.S. Army Engineer Waterways Experiment Station.
- Smith, R.B. (1975) "Seismicity and Earthquake Hazards of the Wasatch Front, Utah," Hearing before the Committee on Aeronautical and Space Sciences, United States Senate, 94th Congress, U.S. Government Printing Office, Washington, D.C.
- Thompson, G.A., Zoback, M.L. (1979) Regional Geophysics of the Colorado Plateau, Tectonophysics, 61(No. 1-3):149-181.
- Wallace, T.C., HelMBERGER, D.V., and Mellman, G.R. (1981) A Technique for the Inversion of Regional Data as Source Parameter Studies, J. Geophys. Res., 86(No. B3):1679-1685.
- Wu, F.T. (1983) A ground motion synthesis study using small earthquakes as Green's functions, Conference on Earthquake Hazards, Beijing, China.
- Yoshikawa, S., Kitano, T., Iwasaki, Y.T., and Tai, M. (1985) Prediction of strong ground motion by synthesis of small events records and site spectral ratio, Tokyo, Japan.